Acta Mechanica Slovaca **28 (1): 26 - 36,** March **2024**
https://doi.org/10.21496/ams.2024.005

Acta Mechanica Slovaca
ISSN 1335-2393
www.actamechanica.sk

Comprehensive Investigation of Solar Water Heater System Performance, Stratification, Charging, and Discharging Efficiency Using TRNSYS Software

Hanane Berrebah [1,*], Touhami Baki [1], Mohamed Tebbal [1]

[1] Faculty of Mechanics, Gaseous Fuels and Environment Laboratory, USTO-MB, El Mnaouer, BP1505, Bir El Djir 31000,Oran, Algeria

Abstract: A study by dynamic simulation using the TRNSYS software was carried out to visualize the performance of a solar water heater with forced circulation for one year. Thermal needs in domestic hot water for an average family of six people living in the city of Oran in Algeria are covered by solar energy by up to 63%. Parameters such as the angle of inclination, the surface of the solar panel, the storage volume, the heat exchanger's surface, and the flow rate of the solar loop have been optimized. An analysis of the temperature stratification inside the balloon was presented, along with the calculation of charging and discharging efficiency. The influence of the position of the exchanger inside the tank has been shown on the temperature stratification and the charging and discharging efficiency.

Keywords: Solar water heater, solar fraction, TRNSYS, charging efficiency, discharging efficiency

1. Introduction

Expanding economies have led to an increased need for energy resources to carry out domestic and economic activities [1], with global energy consumption increasing exponentially in recent decades, from 8,588.9 million tons (Mtoe) in 1995 to 13,147.3 (Mtoe) in 2015. [2] The continuous use of energy has depleted natural resources such as oil, gas, and coal, and over time it can cause environmental harm like greenhouse emissions and chemical waste. These problems harm human health and have an impact on the environment. [3]

Fossil fuels, nuclear resources, and renewable resources are the three main sources of energy. 4 Renewable energy resource technologies such as solar, wind, hydro, biomass, geothermal, and hydrogen have been introduced due to their low environmental impacts. [5] Wind and solar energy are two sources of clean energy, but their choices depend on weather conditions. [6] Solar energy is largely responsible for the expansion of renewable energy; it is one of the fastest-growing forms of energy in the world. [7]

Solar energy includes photovoltaic solar energy isolated from or connected to the grid and solar thermal energy. [8] For the calculation of models of solar radiation, it is recommended to take the value of the total solar irradiance equal to 1361 W/m^2. [9]

Water heating can be met by electric energy or fossil fuel; however, the solar water heater has the ability to reduce the cost in addition to producing clean and sustainable energy. [10] The most common design is the use of an integrated heat exchanger in the storage tank to transfer the heat from the hot fluid captured in the solar collector to the sanitary water contained in the tank. [11] The solar potential in Algeria is very important; the duration of sunshine exceeds 3000 hours per year and can reach 3500

*** Corresponding author:** Hanane Berrebah, ***E-mail address:*** *hanane.berrebah@univ-usto.dz*

hours per year in the Sahara. [12]

Vengadesan et al [13] reviewed developments in the thermo-economic performance of solar water heating systems, they focused on the design, and modification of thermo-physical properties of heat transfer fluids, integrated storage of thermal energy, and hybrid flat plate solar collector systems, they came to the conclusion that the design and the heat transfer coefficient between the fluid and the absorber tubes are the factors that affect the overall performance of the solar water heater; Sakhaei and Valipour [14] analyzed the effect of design parameters such as thickness, coating of the glass cover, thickness and material of absorber plate, the air gap between absorber plate and cover glass and distance between risers and insulation materials on thermal performance.

Harrabi et al [15] carried out the simulation with TRNSYS of a solar water heater to produce domestic hot water in the Tunisian climate. They were able to evaluate the performance of the system over a daily and monthly period, the energy captured by the panels, and the hourly temperature of the hot water produced. Valdiserri [16] made an energy analysis of a solar water heater for the needs of a house in different European cities by simulating with TRNSYS the installation of a solar water heater with a recirculation loop. The study shows the sizing process of the system, the variation of the solar fraction, and the heat losses.

Baki [17] simulated with TRNSYS the performance of a solar water heater producing hot water for the needs of an average family in Algeria and compared the results obtained between three regions with different climates. Significant performances were shown for the south compared to the north and the highlands. Missoum et al [18] studied the performance of a solar water heater under the climate of Algiers by comparing two tank models, the first with a fully mixed tank and the second with a stratified tank. A parametric analysis of the optimal thermal collector, size of storage tanks, and mass flow shows that the solar fraction of the stratified tank is very large compared to the mixed tank.

Lazreg et al [19] studied the temperature stratification in a solar water heater tank for domestic hot water production needs. By doing the simulation with the TRNSYS code, the temperature of several nodes was followed for a day, and the behavior of the system was analyzed. Baki et al [20] analytically studied a solar water heater by comparing the balance of inputs, outputs, and accumulation at the tank level; the approach was formulated mathematically, which made it possible to determine the powers and the internal temperature of the balloon. Shuhong et al [21] experimentally studied the performance of the position of the exchanger in a storage tank of a solar water heater, as well as the efficiency of charging and discharging. The results show that the position of the exchanger affects performance; differences were observed depending on the position. A simulation with TRNSYS was made and compared to the experimental results.

This article mainly identifies the optimization of the solar water heating system, reducing the use of auxiliary energy, and maximizing benefits by calculating the solar fraction from the powers of the system installed by TRNSYS software for a family of six people living in Oran, Algeria. In this work, we also aim to investigate the effect of exchanger location on thermal performance during charging and discharging.

2. Presentation of the model

The simulation study utilizes TRNSYS version 16 software to model a solar water heater system installed in Oran, Algeria. The hot water produced is used to meet the sanitary needs of an average family of six people living in a detached house.

2.1. Solar loop

The solar water heater is made up of a flat thermal solar panel that captures solar radiation and converts it into heat; a set of pipes forming a closed loop connects the solar panel and the exchanger, and the heat absorbed by the heat transfer fluid is released by the exchanger in the tank. The city water arrives in the tank and heats up in contact with the exchanger; it then exits to the household network. When the heat transmitted to the tank is not sufficient to produce hot water at the threshold of 60°C, the auxiliary heating element is strategically positioned on the top inside the storage tank (Type 60d). A pump allows the forced circulation of the heat transfer fluid; it is regulated to operate when the temperature at the outlet of the panel is high enough compared to the temperature at the bottom of the tank. For more detail, see Fig. 1.

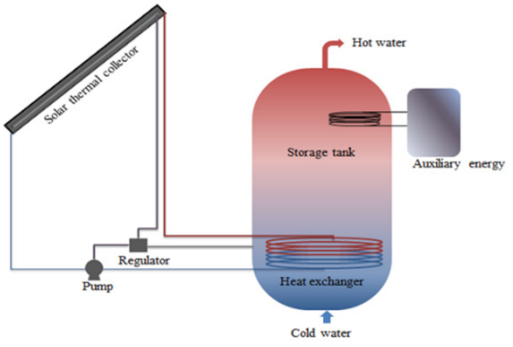

Figure 1: Solar water heater installation.

2.2. Meteorological data

Oran is a coastal city on the edge of the southern shore of the Mediterranean basin; it is located in the northwestern region of Algeria. Its climate is warm temperate, classified Csa (Koppen-Geiger); the winter is cool and humid, and the summer is hot and dry. The average annual temperature is 18 °C, and the average annual irradiation is 840 W/m^2.

Figure 2 shows the variation of the monthly average temperature in Oran; it varies from 11°C to more than 26°C. In January, when it is at its lowest, the temperature is 11°C, then it increases, passes through a peak in July and August with a temperature of 26°C, then decreases to reach 12°C in December. The highest temperature is in the months of July and August, and the lowest temperature is in December, followed by the months of January and February. Fig. 3. Shows the average monthly solar radiation in Oran on an inclined plane of 30°. The flux density varies between 560 W/m^2 at the minimum in December and more than 1000 W/m^2 at the maximum in July, but the irradiation remains significant at 800 W/m^2 or more over the eight months of the year.

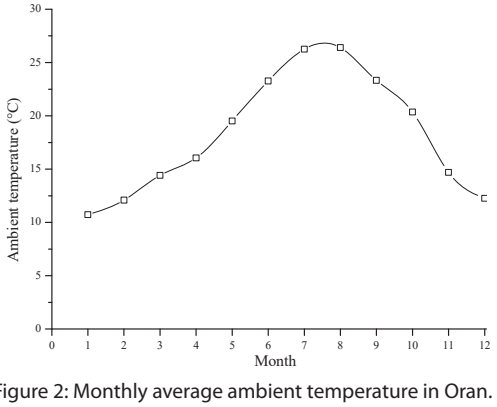

Figure 2: Monthly average ambient temperature in Oran.

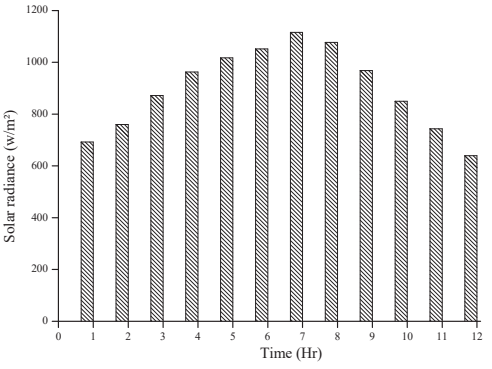

Figure 3: Monthly average solar radiance in Oran.

2.3. TRNSYS schema

TRNSYS is a program used to simulate solar energy applications; it has been marketed since 1975 [22], and it can also be used to evaluate the effect of different design parameters and operating conditions on the performance of the thermosiphon system and forced circulation systems and for the analysis of thermal stratification in the storage tank. TRNSYS version 16 was chosen as the main program in this study because of its diffusion in the field of solar energy and the multiplicity of its fields of use.

Figure 4 illustrates the TRNSYS simulation setup (version 16) specifically adapted for a solar water heating system; the meteorological data are provided by the TMY2 file; the solar loop consists of the Type 60d tank, the Type 1b flat solar thermal collector, the Type 3b pump, and the regulation of the loop will be done by Type 2b; the feed water passes through the Type 14b meter and enters the tank; other elements are added for calculation and data processing. The water supply coil entering tank 60d is regulated by type 14b, and water moves from tank 60d to manifold 1b, which in turn heats the water and moves it to storage 60d, which is switched on and off by type 2b.

2.4. Consumption profile

In residential applications, the demand for domestic hot water varies over time; it can vary from day to day, from season to season, and from family to family. For this study, consumption is 240 liters per day at a temperature of 60°C for a family of six people. The fraction of consumption per hour adapted from [23] is shown in Figure 5; the profile is variable and reaches peaks of 10% in the early morning and the evening; the rest of the day it oscillates between 0, 2, and 4%.

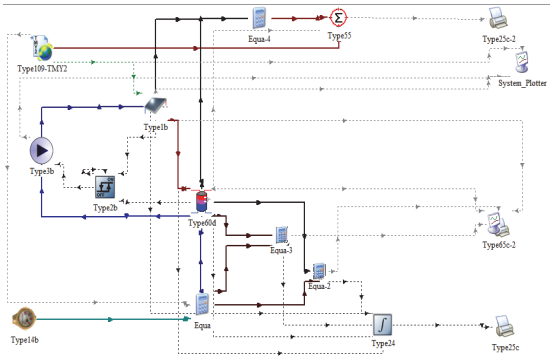

Figure 4: TRNSYS schema.

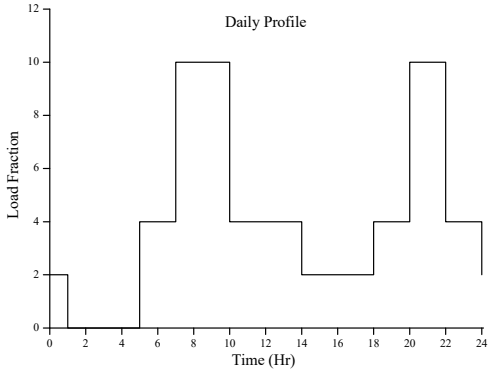

Figure 5: Hot water profile.

2.5. Mathematical formulation

In order to define the parameters used, we present the retained formulations from [24] for the calculation of the variables.

The energy consumed for the production of hot water is determined by:

$$Q_c = \int \dot{f} \dot{m} c_p \left(T_{t,o} - T_{t,i}\right).dt \quad (1)$$

The performance of the flat thermal panel is calculated by:

$$\eta_t = \eta_0 - a_1 \frac{\Delta T}{G} - a_2 \left(\frac{\Delta T}{G}\right)^2 \quad (2)$$

With η_0 being the optical conversion coefficient of the panel (0.8), a_1 representing the heat loss coefficient by conduction of the panel (3.61 W/m^2.K) and a_2 is the heat loss coefficient by convection of the panel (0.0138 W/m^2.K^2).

The useful energy recovered from the thermal panel:

$$Q_u = \int \eta_t A_p G.dt \quad (3)$$

The energy lost by the walls of the balloon:

$$Q_w = \int K_b.A_b \left(T_i - T_L\right).dt \quad (4)$$

The auxiliary energy needed to keep the tank at 60°C:

$$Q_{aux} = Q_w + Q_c - Q_u \quad (5)$$

The solar fraction is:

$$SF = \frac{Q_c - Q_{aux}}{Q_c} \quad (6)$$

Solar fraction is the best indicator of system performance compared to other parameters such as collector efficiency or heat removal factor, as it manifests the overall performance of the whole system [15]. It is defined as the percentage of the total heat load satisfied by solar energy.

To study charging and discharging efficiency, definitions have been retained from. [21] Charging efficiency is the ratio of the average temperature difference; it was introduced to analyze the charging performance of a water tank and is defined by:

$$\varepsilon = \frac{T_{ev}\left(t_h\right) - T_{ev,0}}{T_{e,i}\left(t_h\right) - T_{ev,0}} \quad (7)$$

$T_{ev}(t_h)$ is the storage tank's average temperature, and it is expressed as:

$$T_{ev}\left(t_h\right) = \frac{\sum_{j=1}^{N} T_j\left(t_h\right)}{N} \quad (8)$$

The discharging efficiency was defined as the ratio of energy released to the initial energy stored, and it is equal to:

$$\eta_d = \frac{Q_d\left(t_d\right)}{Q_{e,d}\left(t_d\right) + Q_{d,0}\left(t_d = 0\right)} \quad (9)$$

Where $Q_d(t_d)$ is the energy released, it may be expressed by:

$$Q_d\left(t_d\right) = \vartheta_{use}\, \rho C_p\, \Delta t \sum_{n=1}^{\frac{t_d}{\Delta t}} \left(T_{t,o}\left(t_d\right) - T_{t,i}\right) \quad (10)$$

$Q_{d,0}(t_d=0)$ is the initial energy stored inside the water tank, defined by:

$$Q_{d,0}\left(t_d = 0\right) = V_j\, \rho C_p \sum_{j=1}^{N} \left(T_j\left(t_d = 0\right) - T_{d,i}\right) \quad (11)$$

$Q_{e,d}(t_d)$ is the energy of the heat exchanger, defined by:

$$Q_{e,d}\left(t_d\right) = \vartheta_e\, \rho C_p\, \Delta t \sum_{n=1}^{\frac{t_d}{\Delta t}} \left(T_{e,i}\left(t_d\right) - T_{e,o}\left(t_d\right)\right) \quad (12)$$

3. Maximization of the solar water heater performance

In order to have maximum performance, we study the effects of the parameters on the solar fraction; the choice of the optimal parameter will be the one whose solar fraction is best suited.

3.1. Collector tilt angle

Figure 6. shows the effect of the collector inclination angle on the performance of the solar water heater. If the collector is horizontal the fraction is 0.44, and when the tilt increases the solar fraction increases, passing through the peak between 30° and 40° exactly at 35° where the solar fraction is at its maximum which is 0.633, and then decreasing.

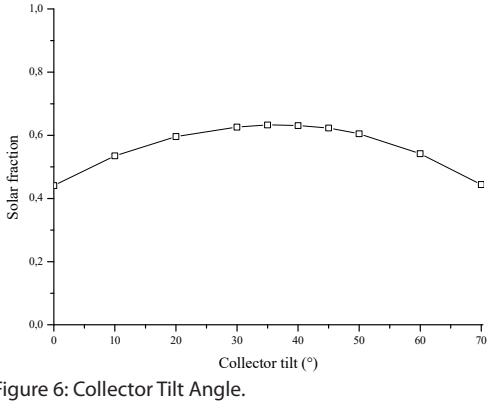

Figure 6: Collector Tilt Angle.

3.2.Collector area

The effect of the solar collector surface on the solar water heater's performance is presented in figure 7. When the surface increases from 1 to 4 m^2, the solar fraction increases consequently, beyond 4m^2 the increase in the fraction is low, then it tends towards a limit around 0.9; similarly, when the surface is greater than 4m^2, the temperature inside the tank exceeds 90°C during the summer; we recommend an area of 4 m^2. Table 1 summarizes the characteristics of the thermal solar collector, including the collector area, inclination, optical conversion coefficient, and the heat loss coefficients via conduction and convection. These parameters are crucial for the system's efficiency.

3.3. Storage tank volume

Fig. 8. Analyzes the influence of the tank volume reported to the surface of the thermal collector on the solar water heater's performance. The solar fraction increases rapidly from 0.49 to 0.63 when the volume ratio parameter on the surface goes from 25 to 75 l/m^2, then the solar fraction becomes almost stable after this value. Our choice falls on the value of 75l/m^2, which gives a volume of 300 liters.

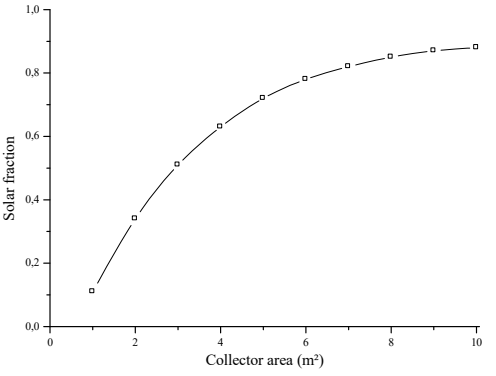

Figure 7: Influence of the Collector area.

Table 1: Characteristics of the Flat Thermal Solar collector.

Thermal solar collector	Value
Collector area	4 m^2
Collector inclination	35°
Optical conversion coefficient	0.8
Heat loss coefficient by conduction	3.61 W/m^2.K
Heat loss coefficient by convection	0.0138 W/m^2.K^2

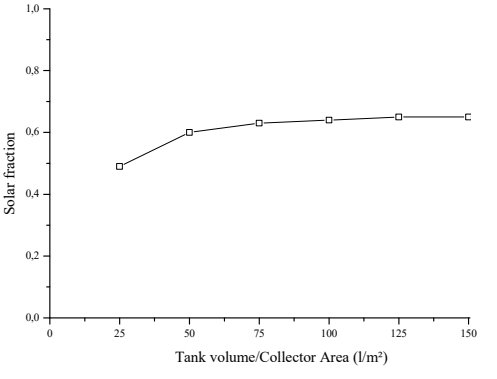

Figure 8: Influence of the storage tank volume.

3.4. Heat exchanger area

The heat exchanger is integrated into the tank; it consists of a tube with an external diameter of 12 mm forming a helical coil of several turns. The exchange surface is that located outside the tube, determined by the product of the perimeter of the outside diameter and the length. The influence of the heat exchanger's exchange surface on the solar fraction is shown in Fig. 9., the performance increases when the surface increases from 0.2 to 1 m^2 then tends towards a limit value, the adequate

value, in this case, is that of 1 m^2.

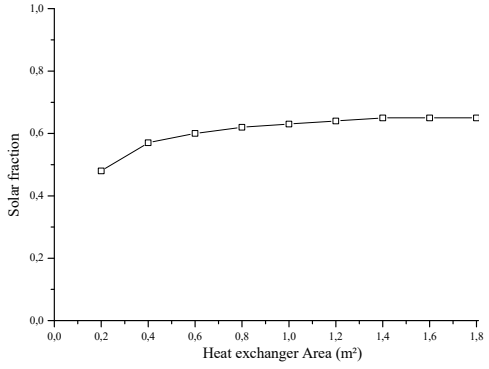

Figure 9: Influence of the heat exchanger area.

3.5. Solar loop mass flowrate

Fig. 10. shows the effect of the mass flow reported on the surface of the thermal collector over a margin of 5 to 45 kg/m^2.h on the solar water heater's performance; when the parameter varies from 5 to 25, the solar fraction quickly increases from 0.47 to 0.63; beyond this value, the solar fraction continues to increase but very slowly until it remains almost constant. After the results, it was noticed that after 25 Kg/m^2.h there was no significant effect on the system. Thus, the mass flow rate of the most appropriate collector would be 25 Kg/m^2.h or 100 Kg/h.

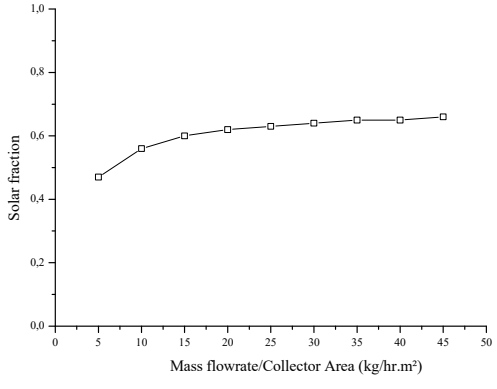

Figure 10: Effect of the collector flow rate.

3.6. Energies useful, auxiliary, and consumption

After examining the results of the effect of the parameters influencing performance, the choice was made for a solar water heater producing domestic hot water at 60°C for an average family of 6 people whose consumption is 240 liters per day on a 4 m^2 thermal panel inclined at 35° and facing the great south, a 300-liter tank, an exchanger surface area of 1 m^2, and a mass flow rate of the loop solar of 100 kg/h.

Fig.11. shows the variation of consumption, useful, and auxiliary energies during a year, the consumption energy remains stable with a slight variation from one month to another, and the useful energy produced by the thermal panel increases from January to July and then decreases after August, and the auxiliary energy makes it possible to make up the deficit between consumption and the useful energy, for this in the cold months the value of the auxiliary energy is at its maximum and decreases in the summer months.

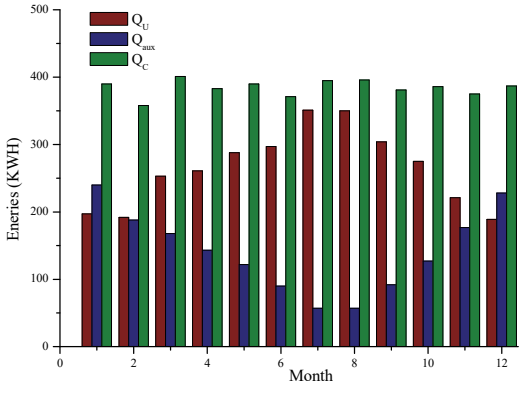

Figure 11: Variation of energies versus the month.

3.7. Solar fraction

The monthly solar fraction is shown in Fig.12. In January it was at its lowest with a value of around 40%. It increases until July and August when it reaches a peak of 86%, then it decreases until it reaches 40% in December. The annual average value is 63%.

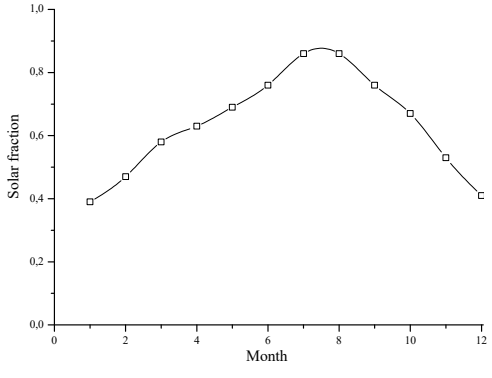

Figure 12: Variation of energies versus the month.

4. Stratification, charging and discharging efficiency

Thermal storage stratification is an important and essential process in the hot water storage tanks study is given by transient temperature profiles under different thermal fluid dynamics conditions. The hot water is in the upper part of a stratified storage tank and the cold water in the lower part of the tank [25].

4.1. Tank nodes

Fig.13. shows a vertical hot water storage tank, with a capacity of 300 liters, a diameter of 0.553 m, and a height of 1.25 m. It is divided into six layers and each layer has an average temperature. The distance between two layers is 0.24m.

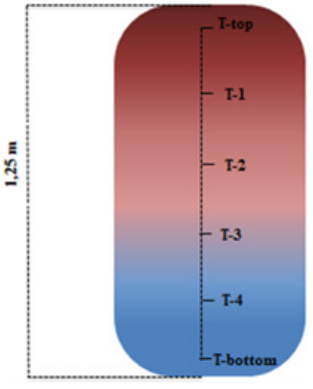

Figure 13: Stratification schema.

4.2. Heat exchanger position

Regarding the position of the heat exchanger within the storage tank, it's important to note that the heat exchanger is indeed situated inside the tank. Fig.14. shows the position of the exchanger inside the storage tank. The exchanger is a copper tube with a diameter of 12 mm and a length of more than 26 m, which applies to an exchange surface of one square meter. The copper tube is coiled with a helical shape with a height of 0.4 m. Three cases of exchanger positioning are studied: low, middle, and high positions. Table 2 details precisely the parameters of the heat exchanger, such as height, diameter, volume and tank water's temperature. Also the position of the heat exchanger inside the tank.

Table 2: Parameters of the Storage Tank and Heat Exchanger System.

Storage tank	Height	1.25 m
	Volume	300 l
	Diameter	0.553 m
	tank water's temperature	60°C
Heat exchanger	Height	0.4 m
	Diameter	0.012 m
	Length	26.54 m
	HX position	Top 0.825/1.125 m
		Middle 0.425/0.825 m
		Bottom 0.025/0.425 m

4.3. Weather data

An analysis of meteorological data from the TMY2 file of the city of Oran allowed us to determine two days where the average temperature was recorded as being the coldest day on January 15 with a temperature of 8.32°C and the hottest day on August 17 with an estimated temperature of 29.72°C. Fig.15. shows the evolution of temperature during the hottest and coldest days. The shape of the two curves is similar, with a shift of around 20°C.

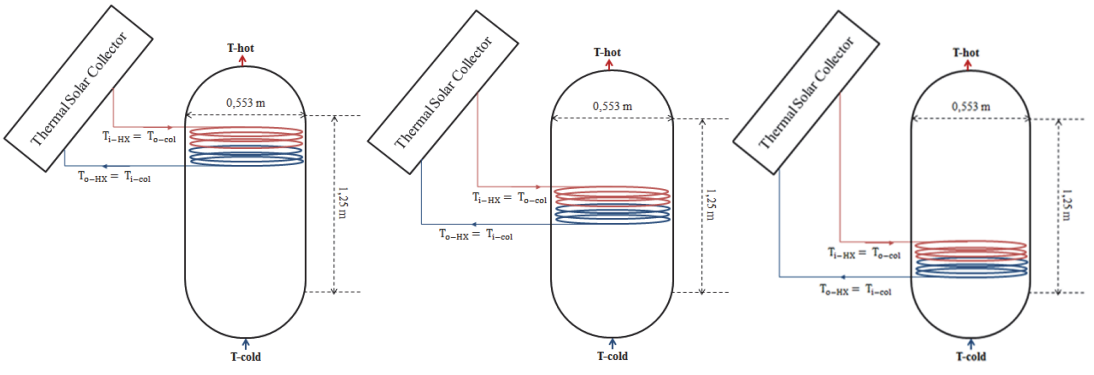

Figure 14: Different HX positions inside a storage tank.

The temperature decreases and then increases until it reaches a peak and then decreases. Fig.16. shows the solar radiation levels on the coldest and hottest days. The radiation level is the same, but the sunshine duration is longer on the day of August 17 than that on the day of January 15; the maximum is reached around 2 p.m.

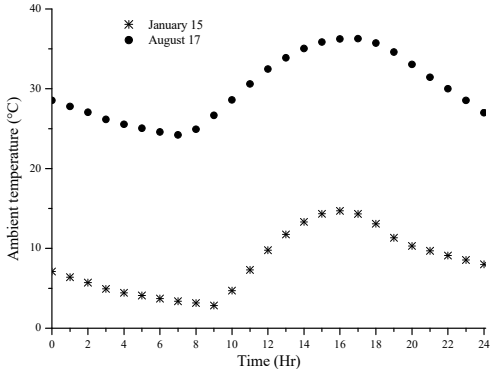

Figure 15: Temperature Evolution Comparison on the Coldest and Hottest Day.

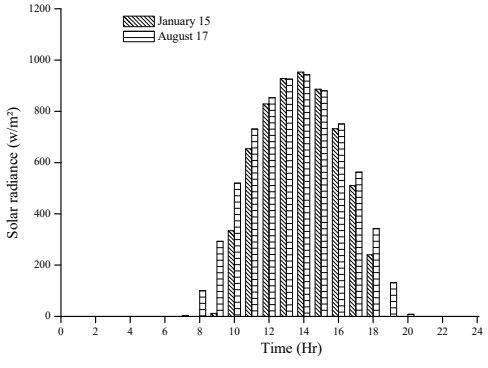

Figure 16: Comparison of radiation levels on the coldest and hottest day.

4.4. Average water temperature inside the tank

The average water temperature for a cold and a hot day chosen from the weather data at TRNSYS software was studied in fig.17 with the varying position of the heat exchanger. All curves have the same distinct shape. During 12 a.m. to 11 a.m., the temperature gradually falls; it rises from 11 a.m. to pass through the peak at 5 p.m. to record the highest temperature, and this is due to the accumulation phenomenon with a huge range of different temperatures between two days. It was also noted that the highest average water temperature was recorded at the bottom-coil position of the heat exchanger, with 47.6 °C and 66.7°C on January 15 and August 17, respectively.

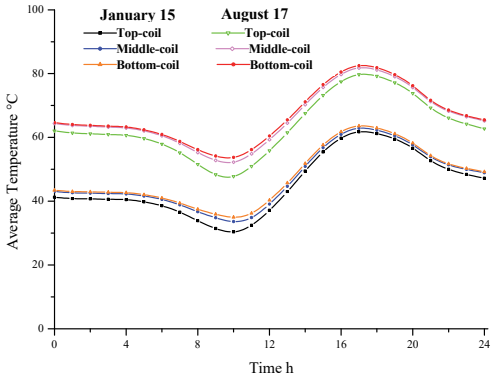

Figure 17: Average water temperature on the coldest and the hottest day inside the tank.

4.5. Temperature stratification

Fig.18. shows the stratification layers inside the reservoir for the coldest day and the hottest day. The strata levels are offset from each other, joined, and then separated.

As sunrise approaches, particularly after 9 am, the temperature inside the tank increases due to heat input from the solar collector. This causes the temperature strata to converge, reducing the temperature difference between them. In the afternoon, as solar radiation decreases and consumption increases, the curves of temperature strata separate.

And from 12 p.m. to 6 p.m., any rise in temperature is caused by the flow rates of hot water from the collector, absorbed by the energy of solar radiation, reaching a peak at 6 p.m. above 60°C on January 15, while exceeding 83°C on August 17 due to the accumulation phenomenon. After 6 p.m., the temperatures drop due to the absence of solar radiation and the existence of temperature differences inside and outside the water tank.

4.6. Charging efficiency

After calculating the water tank's charging efficiency according to equation 07, the results are shown in Fig.19. The charging performance of bottom-coil water is better than middle-coil and top-coil tank positions, which recorded 64% and 71% on January 15 and August 17, respectively, with a difference of 10% and 21% between bottom-coil and top-coil. Compared with a study on the performance of storage tanks in solar water

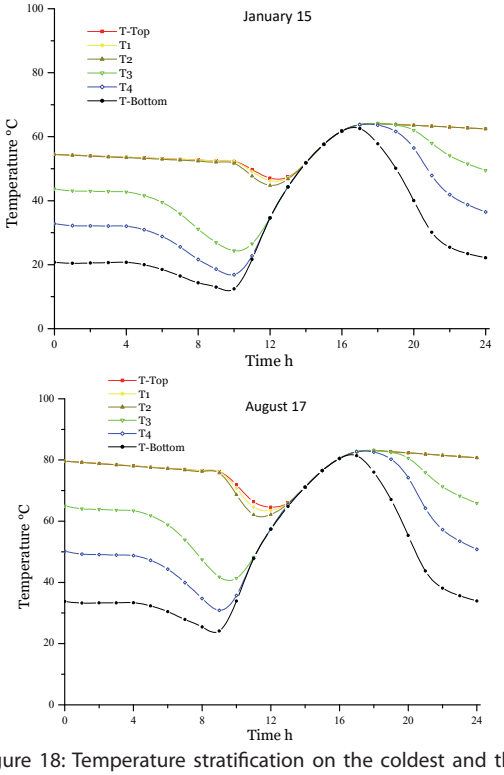

Figure 18: Temperature stratification on the coldest and the hottest day inside the tank.

heater systems in charge and discharge progress by researcher [21], they also found that the best charging efficiency was for the bottom-coil position, with a difference of more than 30% with the top-coil position.

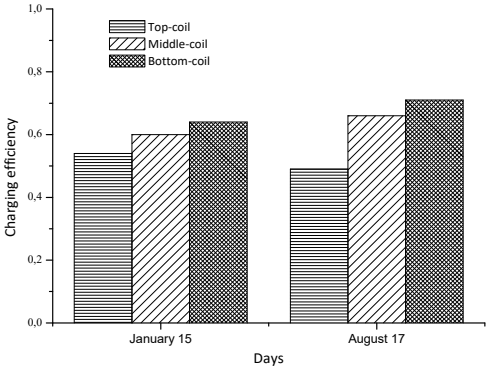

Figure 19: Charging efficiency on the coldest and hottest day.

4.7. Discharging efficiency

After calculating the water tank's discharging efficiency in the case without auxiliary energy, the results are shown in Fig.20. The discharging efficiency is weak on January 15, with almost nonexistent variation not exceeding 1% between heat exchanger positions.

On August 17, the discharging performance of bottom-coil water was better than other positions, with a slight difference of 6% maximum between the bottom-coil and top-coil positions. [21], found in a study on the performance of storage tanks in solar water heating systems that the discharge efficiency of the top-coil was 13.1% higher than the bottom-coil, their study relied on an electrical heater in its installation rather than a thermal solar collector. The flow rate has a low impact on efficiency.

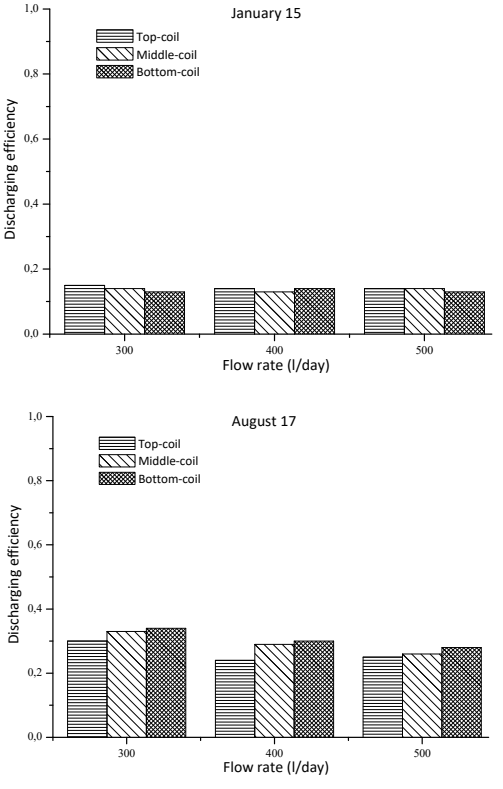

Figure 20: Discharging efficiency on the coldest and hottest day.

5. Conclusions

The analysis of the performance of a solar water heater by a simulation with TRNSYS allowed us to optimize the parameters of influence to arrive at an average annual solar fraction of 63%.

The characteristics derived for the water heater include a panel inclination of 35° with a surface area of 4 m^2, a storage tank volume of 300 liters, an exchange surface area of 1 m^2 situated within the tank, and a solar loop mass flow rate of 100 kg/h.

Considering the thermal energy requirements for domestic hot water, which approximate to 400 kWh per month, and the solar energy supply varies from 200 kWh in January to 350 kWh in July, the difference is made up by the auxiliary electrical energy. Throughout the year, the monthly average solar fraction fluctuates, reaching 40% in colder months and exceeding 80% during warmer periods. Notably, the annual average fraction stabilizes at 63%. The average temperature within the tank varies throughout the day; the peak is obtained around 4 to 5 p.m. The position of the exchanger influences the average temperature by a few degrees. Observations of temperature stratification within the tank reveal maximal temperatures occurring overnight, followed by a sharp decline during the accumulation of solar energy from 1 p.m. to 4 p.m. charging efficiency stands at 63% and 71% for the coldest and hottest days, respectively, with the position of the exchanger impacting overall efficiency by approximately 10 to 20%. Conversely, discharge efficiency registers at 15% and 30% for the coldest and hottest days, respectively, with minimal influence from the exchanger's position, affecting less than 1% of efficiency.

Nomenclature

SF	-	*Solar fraction*
Q_c	W	*Consumption energy*
Q_u	W	*Useful energy*
Q_w	W	*Loss energy by the tank walls*
Q_{aux}	W	*Auxiliary energy*
η_t	-	*Flat thermal panel efficiency*
ε	-	*Charging efficiency*
η_d	-	*Discharging efficiency*
Q_d	W	*Energy released during discharging process*
$Q_{(e,d)}$	W	*Energy of heat exchanger*
$Q_{(d,0)}$	W	*Initial energy stored inside the water tank*
f	-	*Consumption profil fraction*
m	Kg/s	*Mass flowrate*
c_p	J/Kg.K	*Specific heat capacity*
η_0	-	*Optical conversion coefficient of the panel*
a_1	W/m^2.K	*Heat loss coefficient by conduction of the panel*
a_2	W/m^2.K^2	*Heat loss coefficient by convection of the panel*
G	W/m^2	*Solar radiance*
A_p	m^2	*Panel area*
K_b	W/m^2.K	*Heat transfer coefficient by convection*
A_b	m^2	*Tank area*
ϑ_{use}	m^3/s	*Volume flow rate during discharging*
V_j	m^3	*Volume of layer j*
ϑe	m^3/s	*Volume flow rate of heat exchanger*
N	-	*Layers' number*
$T_{(t,o)}$	K	*Outlet temperature of the water tank*
$T_{(t,i)}$	K	*Inlet temperature of the water tank*
T_i	K	*Temperature inside the water tank*
T_L	K	*Local temperature*
T_{ev}	K	*average initial water temperature in the storage tank*
$T_{(e,i)}$	K	Heat exchanger inlet temperature
$T_{(e,o)}$	K	Heat exchanger outlet temperature
T_j	K	water temperature of layer j

References and Notes

1. Dorahaki, S., Rashidinejad, M., Abdollahi, A., & Mollahassanipour, M. (2018). A novel two-stage structure for coordination of energy efficiency and demand response in the smart grid environment. International Journal of Electrical Power & Energy Systems, 97, 353-362.
2. Ahmad, T., & Zhang, D. (2020). A critical review of comparative global historical energy consumption and future demand: The story told so far. Energy Reports, 6, 1973-1991.
3. Chien, F., Huang, L., & Zhao, W. (2023). The influence of sustainable energy demands on energy efficiency: Evidence from China. Journal of Innovation & Knowledge, 8(1), 100298.
4. Qazi, A., Hussain, F., Rahim, N. A., Hardaker, G., Alghazzawi, D., Shaban, K., & Haruna, K. (2019). Towards sustainable energy: a systematic review of renewable energy sources, technologies, and public opinions. IEEE access, 7, 63837-63851.
5. Ang, T. Z., Salem, M., Kamarol, M., Das, H. S., Nazari, M. A., & Prabaharan, N. (2022). A comprehensive study of renewable energy sources: classifications, challenges and suggestions. Energy Strategy Reviews, 43, 100939.
6. Campos-Guzmán, V., García-Cáscales, M. S., Espinosa, N., & Urbina, A. (2019). Life Cycle Analysis with Multi-Criteria Decision Making: A review of approaches for the sustainability evaluation of renewable energy technologies. Renewable and Sustainable Energy Reviews, 104,343-366.
7. McCall, J. (2020). Turning Toward the Sun: A Cross-National Analysis of Solar Energy Generation. International Journal of Sociology, 50(4), 310-324.
8. Bortoluzzi, M., de Souza, C. C., & Furlan, M. (2021). Bibliometric analysis of renewable energy types using key performance indicators and multicriteria decision models. Renewable and Sustainable Energy Reviews, 143, 110958.
9. Almorox, J., Voyant, C., Bailek, N., Kuriqi, A., & Arnaldo, J. A. (2021). Total solar irradiance's effect on the performance of

empirical models for estimating global solar radiation: An empirical-based review. Energy, 236, 121486.
10. Koroneos, C. J., & Nanaki, E. A. (2012). Life cycle environmental impact assessment of a solar water heater. Journal of Cleaner Production, 37, 154-161.
11. Knudsen, S., & Furbo, S. (2004). Thermal stratification in vertical mantle heat-exchangers with application to solar domestic hot-water systems. Applied Energy, 78(3), 257-272.
12. Gairaa, K., Khellaf, A., Benkacilai, S., & Guermoui, M. (2017). Solar radiation measurements in Algeria: case of Ghardaïa station as member of the enerMENA meteorological network. Energy Procedia, 141, 50-54.
13. Vengadesan, E., & Senthil, R. (2020). A review on recent development of thermal performance enhancement methods of flat plate solar water heater. Solar Energy, 206, 935-961.
14. Sakhaei, S. A., & Valipour, M. S. (2019). Performance enhancement analysis of the flat plate collectors: a comprehensive review. Renewable and Sustainable Energy Reviews, 102, 186-204. DOI: 10.1016/j.rser.2018.11.014
15. Harrabi, I., Hamdi, M., Bessifi, A., & Hazami, M. (2021). Dynamic modeling of solar thermal collectors for domestic hot water production using TRNSYS. Euro-Mediterranean Journal for Environmental Integration, 6, 1-17.
16. Valdiserri, P. (2018). Evaluation and control of thermal losses and solar fraction in a hot water solar system. International Journal of Low-Carbon Technologies, 13(3), 260-265.
17. Baki, T. (2021). Comparison of the performance of a domestic solar water heater in different climates in Algeria. Present Environment & Sustainable Development, 15(1), 143-151.
18. Missoum, M., Hamidat, A., Imessad, K., Bensalem, S., & Khodja, A. (2016, March). Energy performance investigation of a solar water heating system for single-family houses in Mediterranean climate. In 2016 7th International Renewable Energy Congress (IREC) (pp. 1-6). IEEE.
19. Lazreg, M., Baki, T., & Nehari, D. (2020). Effect of Parameters on the Stratification of a Solar Water Heater. In ICREEC 2019: Proceedings of the 1st International Conference on Renewable Energy and Energy Conversion (pp. 117-125). Springer Singapore.
20. Baki, T., Tebbal, M., & Berrebah, H. (2021). Following the balloon temperature of a solar heater installed in Oran, Algeria. Turkish Journal of Electromechanics & Energy, 6(2), 73-79.
21. Shuhong Li, Yongxin Zhang, Kai Zhang, Xianliang Li, Yang Li, Xiaosong Zhang, Study on Performance of Storage Tanks in Solar Water Heater System in Charge and Discharge Progress, Energy Procedia, Volume 48, 2014, Pages 384-393.
22. Džiugaitė-Tumėnienė, R., & Streckienė, G. (2014, May). Solar hot water heating system analysis using different software in single family house. In The 9th International Conference "Environmental Engineering", 22–23 May 2014, Vilnius, Lithuania (p. 9).
23. Baki, T., Sandid, A. M., & Nehari, D. (2022). Sizing of an Autonomous Individual Solar Water Heater Based in Oran, Algeria. Slovak Journal of Civil Engineering, 30(3), 9-16.
24. Baki, T., & Madjber, H. (2022). Assessment of the Thermal and Electrical Energy Needs of an Autonomous Single-Family House. Journal of Electrical and Electronics Engineering, 15(1), 9-14.
25. Madhlopa, A., Mgawi, R., & Taulo, J. (2006). Experimental study of temperature stratification in an integrated collector–storage solar water heater with two horizontal tanks. Solar Energy, 80(8),989-1002.